Fuel Cell Electric Vehicle-to-grid feasibility

A technical analysis of aggregated units offering frequency

Robledo, Carla; Poorte, M.J.; Mathijssen, H.H.M.; van der Veen, Reinier; van Wijk, Ad

DOI
10.1007/978-3-030-00057-8_8

Publication date
2019

Document Version
Final published version

Published in
Intelligent Integrated Energy Systems

Citation (APA)
Robledo, C., Poorte, M. J., Mathijssen, H. H. M., van der Veen, R., & van Wijk, A. (2019). Fuel Cell Electric Vehicle-to-grid feasibility: A technical analysis of aggregated units offering frequency. In P. Palensky, M. Cvetkovic, & T. Keviczky (Eds.), *Intelligent Integrated Energy Systems: The PowerWeb Program at TU Delft* (pp. 167-194). Springer. https://doi.org/10.1007/978-3-030-00057-8_8

Chapter 8
Fuel Cell Electric Vehicle-to-Grid Feasibility: A Technical Analysis of Aggregated Units Offering Frequency Reserves

C. B. Robledo, M. J. Poorte, H. H. M. Mathijssen, R. A. C. van der Veen and A. J. M. van Wijk

Abstract Fuel Cell Electric Vehicles (FCEVs) in combination with green hydrogen (obtained from renewable sources), could make a significant contribution in decarbonizing the European transport sector, and thus help achieve the ambitious climate goals. However, most vehicles are parked for about 95% of their life time. This work proposes the more efficient use of these vehicles by providing vehicle-to-grid (V2G) services achieving the integration of the transport and energy systems. The aim of this work is to determine the technical and financial potential value that FCEVs could have by providing frequency reserves. Experiments were carried out with a Hyundai ix35 FCEV that was adapted with a power output socket so it can operate in V2G when parked, delivering maximum 10 kW direct current power. Results show that both power sources in the fuel cell electric vehicle, which are the fuel cell stack and the battery, can react in the order of milliseconds and thus are suitable to offer fast frequency reserves. The challenge lays in the communication between the car and the party that sends the signal for the activation of the frequency reserves. As one

C. B. Robledo (✉)
Process and Energy, 3mE, Delft University of Technology, Leeghwaterstraat 39, 2628CB Delft, The Netherlands
e-mail: c.b.robledo@tudelft.nl

M. J. Poorte
Talent voor Transitie, Bergstraat 35, 6811LC Arnhem, The Netherlands
e-mail: michelle.poorte@talentvoortransitie.nl

H. H. M. Mathijssen
TenneT, Utrechtseweg 310, 6812AR Arnhem, The Netherlands
e-mail: Henrie.Mathijssen@tennet.eu

R. A. C. van der Veen
CE Delft, Oude Delft 180, 2611HH Delft, The Netherlands
e-mail: veen@ce.nl

A. J. M. van Wijk
Process and Energy, 3mE, Delft University of Technology, Leeghwaterstraat 39, 2628CB Delft, The Netherlands
e-mail: a.j.m.vanwijk@tudelft.nl

P. Palensky et al. (eds.), *Intelligent Integrated Energy Systems*,
https://doi.org/10.1007/978-3-030-00057-8_8

unit does not provide enough power to be able to participate in the electricity market, a car park acting as aggregator of FCEVs was designed taking into account current technology developments. A carpark with a direct current microgrid, a hydrogen local network and only occupied by FCEVs was designed. A financial model was developed to evaluate the economic potential of the car park to participate in the electricity market providing frequency reserves. Results show that by using the fuel cells in the FCEVs in V2G, monetary benefits could be obtained when providing automated frequency restoration reserves (aFRR) upwards. Key parameters are found to be the investment costs, amount of vehicles available, hydrogen price and price of aFRR. With a car park of approximately 400 cars all year long available, payback times of 11.8 and 3.5 years were obtained taking into account worst and best case scenarios for a 15 year period analysis, respectively.

8.1 Introduction

In the process of liberalization of the electricity market in Europe that took place in the late 1990s, the electricity industry has become a competitive market, where different entities belonging to the Distribution System Operators (DSOs) and Transmission System Operators (TSOs) bear responsibility for the operation and security of the power system [1]. Users connected to the power system expect that the frequency and voltage stay close to their nominal values in order to ensure that their electronic devices will operate correctly. The frequency of the power system is used as an indicator of the (im)balance between the generation and the demand of the total active power in the system. Therefore, frequency control represents a crucial part of ancillary services [2]. Since the undergoing process of the electricity market and the increase of intermittent generation, the European power system has been exposed to high and persisting frequency deviations [1]. This is mainly due to the increase in the electricity production mix of wind and solar power, driven by the energy transition to a more sustainable power system [3, 4]. New and innovative technologies will have to be implemented in the current system in order to cope with the environmental needs and to secure constant electricity supply in the future energy system.

Electric vehicles (EVs) with vehicle-to-grid (V2G) technology have the capability to provide electricity to the grid, and have thus the potential to join the electricity market in providing ancillary services [5, 6]. Personal vehicles are utilized only 5% of their lifetime for transportation. The remaining time they can be used for a secondary function, like offering frequency reserves [7]. However, the individual participation of single EVs as electricity providers is not possible for mainly two reasons. First, the individual capacity is too small to participate in power system markets and second, the availability of one single EV is unpredictable from the power system's perspective as its main purpose is transportation. A larger fleet of vehicles could provide a solution by delivering a significant amount of reserves to the power system, while being more reliable. Such a mechanism to form clusters of smaller single units, that together could offer services, is called aggregation and is administered by the aggregator [8]. An

aggregator acts as a mediator between the system operator and small-scale customers, enabling mutually beneficial coordination for EV owners and the power system [9]. The key role of the aggregator is to present the dispersed power units as a single cluster to the system operator.

There are mainly three types of EVs that could be used in V2G mode; plug-in hybrid (PHEV), battery (BEV) and fuel cell electric vehicles (FCEV) [10]. BEVs can store electricity and deliver it back to the grid when needed, whereas PHEVs and FCEVs can generate electricity from fuel stored on-board or fed into the car. We focus on FCEVs because they provide the only possibility to generate clean electricity, if hydrogen is produced from renewable energy sources. When parked, these cars can produce electricity in a clean and efficient way with only water and heat as by-products [6]. It is expected that future energy networks will allow higher level of interactions between electrical grid, thermal grind and fuel grid with hydrogen as the energy carrier [11]. Hydrogen can become an important energy carrier next to electricity, which can be transported by pipeline, with electrolysers and FCEVs becoming important units for power system balancing. FCEVs can use hydrogen for driving, and for power production when parked. Thus, hydrogen is a potential energy carrier to allow higher interactions between the different energy grids.

Technical capability and potential income generation of V2G services provided with FCEVs are not known yet but essential for the feasibility of FCEV aggregation providing frequency reserves. Therefore, in this chapter we seek to do so in two separate analyses. An experimental approach is used to test the dynamic response of a FCEV connected to the grid and delivering electricity at different power outputs. The second approach consists of the design and financial modeling of a car park, acting as aggregator, to provide several frequency control products in the energy market. We give a brief introduction to the frequency control system in Europe, and in particular on the Dutch system where the experiments were carried out. Also, fundamental aspects of V2G technology and hydrogen fuel cell electric vehicles are addressed.

8.1.1 Dutch Electric Power System

The Dutch electricity network is embedded in the synchronous area (SA) of Continental Europe, which is the largest one in the world and supplies over 400 million customers in 24 countries [12]. The most relevant frequency parameters and targets have been identified and set by the European Network of Transmission System Operators for Electricity (ENTSO-E) to guarantee a secure power system. Within the ENTSO-E network there are five SAs: Continental (CE), Nordic (NE), Baltic, British (BE), and Irish (IRE) Europe. The quality parameters are embedded in formal EU regulation in the System Operation Guideline (SO GL). In Europe, the nominal frequency has been set at 50 Hz. Frequency deviations from this value could lead to a complete blackout if not treated properly in time.

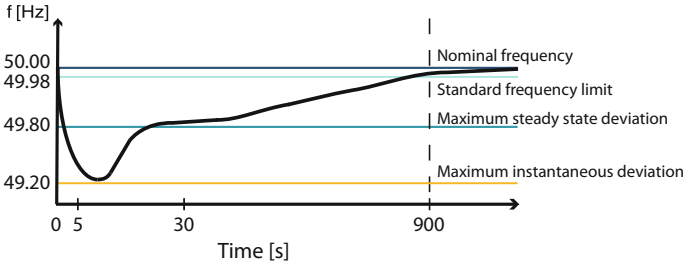

Fig. 8.1 Power system frequency along time after a power generation outage at time 0 [14]

8.1.1.1 Frequency Control

Figure 8.1 shows the dynamic behavior of the frequency after a power generation outage. At the moment of power outage (time = 0), a decrease of the frequency can be noticed. The maximum allowed deviation occurring after an incident is called the maximum instantaneous frequency deviation, which is equal to a deviation of 800 mHz compared to the nominal frequency. The maximum steady state frequency deviation is the limit that the frequency can reach without bringing the stability of the system in danger. The time to restore frequency after a power output indicates the maximum duration of a deviation until the frequency is restored to the standard frequency range (49.98–50.00 Hz) and is equal to 15 min. To bring the frequency back within the standard frequency range a control mechanism called Load Frequency Control (LFC) is established. The mechanism of LFC is a system that can activate power reserves in case of an imbalance. If there is a shortage of power, the frequency reserves can be activated and ramp up; if there is abundance, they can ramp down. In the European system, there are three types of reserves that contribute to the stabilization of the frequency: frequency containment reserves (FCR), frequency restoration reserves (FRR), and replacement reserves (RR). The RR are not used in the Dutch system and will therefore not be considered in this research.

When a disturbance takes place, first the FCR are activated. As a result, the deviation of the frequency stops and stabilizes at a value that differs from the nominal value. Then, FRR are activated to bring the frequency back to its nominal value. The time required to ramp up or down the reserves influences the time it takes to stabilize the frequency. Currently the full activation time (FAT), which is the time to activate the needed reserves, is 30 s for FCR. The FRR must be activated within 15 min (900 s). These time frames are indicated in Fig. 8.1.

The amount of FCR required per TSO is calculated each year based on the share of electricity that is produced and consumed within the operation area of that TSO and the total synchronous area. For the Dutch TSO TenneT, the amount of FCR has been approximately 100 MW in the past years. This reserve must be offered symmetrically, meaning that if 10 MW of FCR are offered, then the power source must be able to both ramp up and ramp down 10 MW.

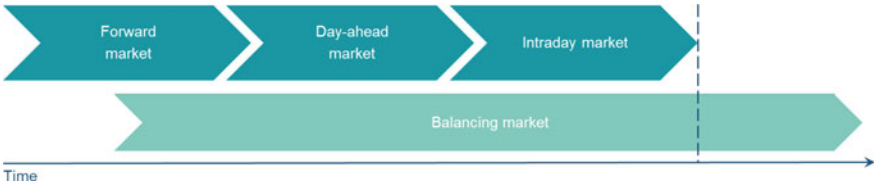

Fig. 8.2 Timeline of the electricity markets. The dotted line indicates the actual moment of electricity transmission

The FRR is used to balance the power to its scheduled value. This process involves automatically instructed services (aFRR), previously known as secondary reserves, and manually instructed services (mFRR), known as tertiary reserves [13]. Currently the required amount of available aFRR in the Netherlands is 340 MW upward and 340 MW downward. These reserves are contracted separately. In this research mFRR, used for large-scale and expected long-lasting imbalances, will not be taken into consideration, as these reserves are subject to long-term contracts and are sporadically used. This makes it less interesting for the small-scale technologies to participate in this market.

8.1.1.2 Market Regulations

The Dutch electricity market can be divided in four submarkets based on the time until the actual electricity production and consumption takes place. Figure 8.2 shows an overview of these four markets in chronological order with respect to the moment of trade delimited as a dotted line. On the forward (or long-term) market the largest share of electricity is sold. This is done with contracts of years, quarters or months. The day-ahead market takes place one day before the actual transmission of electricity. On this market expected changes in production or consumption can be adjusted. This trade takes place by means of an auction. Bids can be done 24 h a day starting 45 days before the delivery day. The auction is open until 12.00 h of the day before transmission. The auction is cleared and a price per hour is determined; this is by the marginal price on the bid ladder [15]. The intraday market opens when the operators of TenneT have checked the balance on the grid, which is usually around 17.00 h of the day before the electricity transmission. It closes 5 min before the actual delivery. This trade also takes place in the form of an auction in blocks of one hour [16]. The fourth market is the balancing market, which is the entirety of institutional, commercial and operational arrangements that establish market-based management of balancing. This includes also the markets for frequency reserves. This market is spread over a larger time frame. FCR is traded before the electricity transmission. However for FRR, there is a bidding, activation and a settlement phase. The first phase occurs before the scheduled electricity is produced, the second phase takes place in real time and the settlement phase takes place after the electricity production.

8.1.1.3 Responsibilities

To manage the activation of the frequency reserves, a cascade of responsibilities, that begin at European level, has been established in the SO GL, which was drafted by ENTSO-E and is official EU regulation since 14 September 2017 [17].

To be able to balance supply and demand, the Dutch law attributes the administrative responsibility of forecasting generation and demand to the balance responsible parties (BRP). During the planning phase, the BRP provides energy-programs (E-programs) to the TSO a day before the day of delivery. An E-program contains the transactions of energy during an imbalance settlement period (ISP). After gate closure time, the BRP have the responsibility to accept the imbalance price in case they have deviated from the scheduled net energy injection or withdrawal [18].

The last relevant actors for the balancing mechanism are the balancing service providers (BSP). These provide the reserves required for balancing. The BSP offer their capacity for a given price on the specific markets for frequency reserves. For the different frequency reserves there are different activation mechanisms.

8.1.2 Fuel Cell Electric Vehicles and V2G

FCEVs store energy in molecular hydrogen H_2, which is fed into a fuel cell along with atmospheric oxygen, producing electricity with heat and water as by-products. Commercially available FCEVs use Proton Exchange Membrane Fuel Cells (PEMFCs) to convert hydrogen into electricity, have a High Voltage (HV) battery connected in parallel and store H_2 in gaseous form at 700 bar [19–22]. This electricity is used to drive the electric motor and also to charge the HV battery. For a moderate power demand, the vehicle feeds only from the fuel cell to power the traction motor. When the vehicle is moving uphill or accelerating, the traction motor is driven by the battery and fuel cell together [23].

Even before the term V2G was introduced in the literature, Kissock analyzed the potential of FCEVs to provide power for buildings and focused primarily on the ability of using waste heat for both space heating and to help operate an absorption cooling system for different buildings [24]. Three years later, Kempton et al. introduced the term V2G and examined the economic potential of using different types of EVs to produce power for buildings and the grid, as well as to provide ancillary services [10]. They concluded that FCEVs could compete in the peak power market but could not compete with baseload power. Lipman et al. assessed the economic benefits from a customer side of stationary fuel cells and FCEVs providing power for residential and commercial use. They concluded that FCEVs used for power in commercial "office building" can potentially supply electricity at competitive rates, in some cases producing significant annual benefits to vehicle owners while at the same time producing additional capacity to utility grids [25]. Also, the FCEVs have been considered to provide balancing power for smart city areas in a 100% renewable energy system [26]. All these relevant studies have analyzed the potential of FCEVs

to provide power for different electricity markets theoretically, and in 2016 the main concept was tested in reality for the first time at the Green Village in The Netherland, the living lab of Delft University if Technology. A commercial FCEV was adapted and was connected to the national Dutch grid, delivering 9.5 kW AC power [27]. This was done within the Car as Power Plant project which entails a vision of an integrated sustainable energy and mobility system, based on renewable energy sources, hydrogen as an energy carrier and FCEVs [6]. A main business case related to the Car as Power Plant concept is that of the Car Park as Power Plant (CPPP), which consists of the aggregation of FCEVs parked in a car park into a 'virtual power plant' to produce electricity and feed it into the power grid [28]. This work elaborates on this existing concept and brings new insights on the use of FCEVs for frequency reserves.

8.2 Methodology

In this chapter we explain the methods employed to analyze the use of aggregated FCEVs to offer frequency reserves. First, the technical capability of a commercial available FCEV to ramp up and down according to FCR requirements was tested. Then, the results were taken as input in a model developed to simulate a car park aggregating FCEVs and taking into consideration the technical characteristics of the cars, relevant actors and the market regulations. Details of both methods are exposed in the following sub-sections.

8.2.1 Technical Evaluation of a FCEV to Provide Power to the Grid

The main objective of the experiment was to estimate the reaction time of the FCEV in V2G mode, which is a key component in estimating the FAT. The FAT stands for the time the balancing resource needs to ramp up from zero to the maximum power output or ramp down from the maximum power to zero. The two frequency reserves taken into consideration are FCR and aFRR. Considering that the FAT for FCR is shorter than that for aFRR, if the FCEV satisfies the requirements for the first, it also satisfies the latter. The FAT is composed of two parts, as shown in Eq. (8.1).

$$FAT = ReactionDelay + ReactionTime \tag{8.1}$$

The reaction delay is the time related to the data communication, which is measured from the moment that a signal is sent by the BRP until the moment that the balancing resource actually reacts. The reaction time of the FAT is the time that the balancing resource actually adjusts the power output and reaches the point of full

activation. As no actual aggregation, control mechanism and communication system is yet available for the CPPP concept, the reaction delay of this aggregation was not measured. During the experiment only the reaction time of the balancing resource was measured and the reaction delay was obtained from a V2G pilot with BEVs in The Netherlands, as this is equal to both type of EVs.

8.2.1.1 Experimental Setup

The tests were carried out at the Car as Power Plant set up located at The Green Village in The Netherlands, shown in Fig. 8.3. The Green Village is a unique platform that unites researchers, entrepreneurs, government and general public to help innovations get to large-scale application [29]. The experimental set-up consisted of mainly three components:

1. The modified Hyundai ix35 FCEV with V2G Direct Current (DC) outlet plug and data monitoring system on-board.
2. V2G unit with inverter inside, that converts DC power in the range of 300-400 V received from the FCEV into three-phase Alternating Current (AC) at 380 V.
3. A three-phase 380 V AC grid connection with galvanic isolation, including fuses and kWh meter.

The Hyundai ix35 FCEV has a 100 kW FC on board, connected to a Li-polymer battery in parallel, that has an energy capacity of 0.95 kWh and a maximum power output and input of 24 kW [30]. It is equipped with a large radiator and cooling

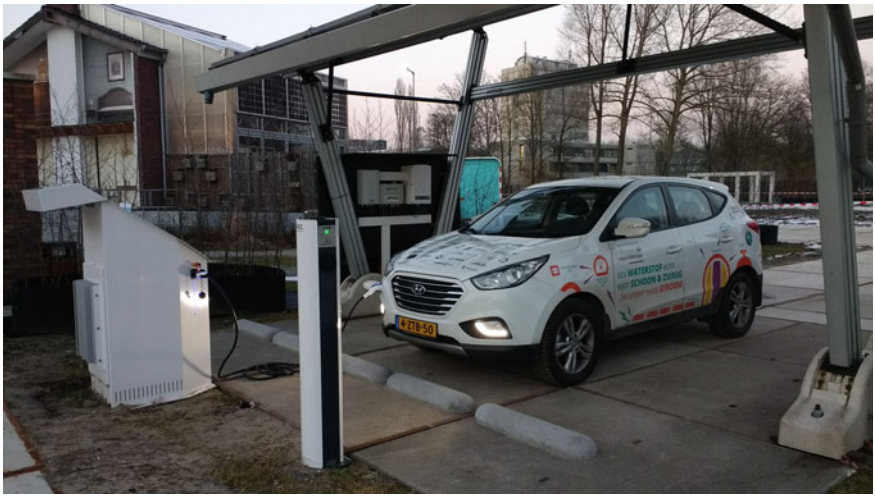

Fig. 8.3 Photo of the modified Hyundai ix35 FCEV connected to the grid through the V2G unit at The Green Village in The Netherlands

fan to maintain the temperature at a desirable operating level. In stationary mode the FCEV has less cooling capacity and cannot operate at the maximum power of 100 kW. For this reason the maximum power output in V2G mode was restricted to 10 kW DC that enables the on-board utilities of the FCEV to regulate the fuel cell's temperature [31]. More specifics about the technical and safety details of the set-up can be found in this reference [26].

8.2.1.2 Measurements

To determine the reaction time of the FCEV connected to the grid, the power output of the FCEV was measured while the inverter at the V2G unit was switched on and off. This was done to simulate when the car would be asked to deliver power by the aggregator in a future CPPP system. While the FCEV was connected to the V2G unit, turned on and not delivering power, it remained in idling condition. Once the inverter in the discharge unit was switched on, the FCEV actively started delivering power. By switching on and off the discharge unit, the FCEV was activated (ramp up) and deactivated (ramp down).

Two different power settings were tested. The first setting was for a power output of 10 kW DC from the car and the second one, a power output of 5 kW DC. As it can be seen in Fig. 8.4, the FCEV was allowed to idle for 2 min, followed by the delivery of power during 5 min. This cycle was repeated 10 times to improve the reliability of the measurements for both settings.

During the experiments, current and voltage was monitored and measured in the fuel cell and battery of the FCEV with a frequency of 5 Hz. The power values were calculated by multiplying the individual current and voltage values. The total DC power output of the FCEV in V2G was equal to the sum of the FC and the battery DC power output. With these values the power gradient ($\Delta P/\Delta t$) was calculated as

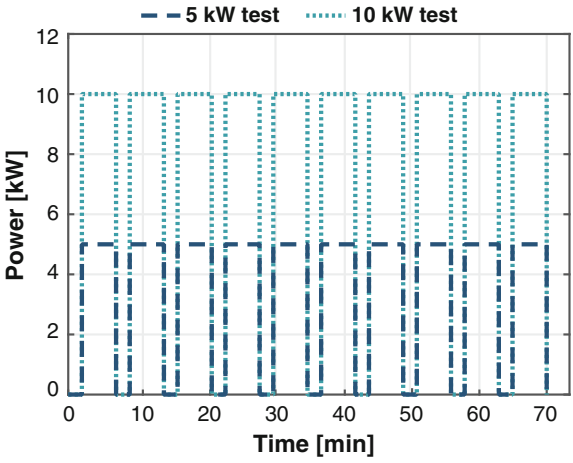

Fig. 8.4 Power input settings during the experiment with the FCEV delivering power in V2G mode

expressed in Eq. (8.2).

$$\frac{\Delta P}{\Delta t} = (P_{t+1} - P_t) \times f \tag{8.2}$$

where P_{t+1} is the power output of battery or FC at time t+1, P_t is the power output at time t, and f is the logging frequency. This was calculated for each cycle and for each component (battery and FC), when ramping up (switching on), as well as ramping down (switching off). The average of these measurements was used as indicator of the reaction time of the FCEV.

8.2.2 Financial Modeling of Car Park with FCEVs Providing Frequency Reserves

The overall scope of the financial analysis is to evaluate for which conditions the net present value (NPV) and the payback time of a CPPP offering frequency reserves are, respectively maximized and minimized. The model evaluates every 15 min of a year, all the combinations of the products that can be offered by the CPPP (electricity, FCR and aFRR) and the related energy that is used to offer these products. A time step of 15 min is chosen, as it is equal to the imbalance settlement period (ISP) of the Dutch power system. To calculate the NPV and the payback time four main steps were performed. First, the total power that can be offered by the car park was calculated. Then, the constraints related to the balancing market were implemented. Thirdly, the revenues and costs were calculated, and finally the yearly profit (calculated with the revenue and costs of the previous step) was used to obtain the NPV and payback time based on investment estimations. In the following two sub-sections the system design and model assumptions are explained.

8.2.2.1 System Design and Assumptions

In order for the concept of CPPP to be feasible, the fleet of FCEVs has to increase with respect to its current level. In 2016 only 31 vehicles were FCEVs within the total amount of 8,222,974 registered vehicles in The Netherlands [32]. We assume that the concept of a car park with FCEVs that operates as a power plant could become feasible from 2030 onwards. This is considering mainly three recent local developments:

1. In 2017, the new Dutch government presented its plans for the coming years and established that by 2030 all produced and sold cars must be emission free. In this category fall only battery and fuel cell electric vehicles.
2. The whitepaper presented by H_2 platform in May 2018 to be incorporated in the climate agreement in The Netherlands. The goal is to increase the amount

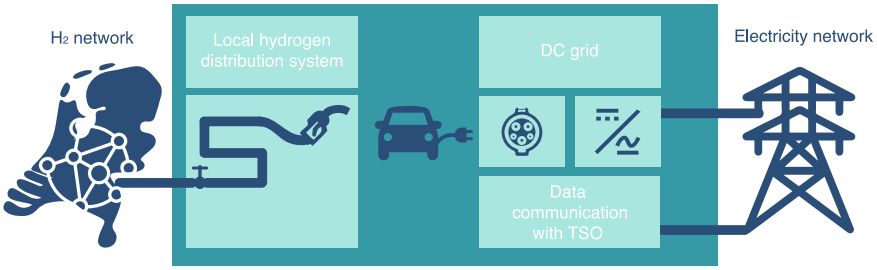

Fig. 8.5 Schematic representation of the CPPP system design with its main components; local hydrogen network, hydrogen dispensing, DC electrical grid in the car park, conversion to AC and data communication components

of FCEVs and Hydrogen fuel stations in The Netherlands to 375,000 and 216, respectively by 2030 [33].

3. EU targets to reduce the amount of CO_2 emitted per km for passenger cars from 130 g CO_2/km in 2015 to 95 g CO_2/km in 2021 and 70 g CO_2/km in 2025 [17].

The demand for hydrogen will rise and not only for its use in transportation, but also to satisfy the heating demand in residential and commercial buildings [34]. For higher demand of hydrogen, large-scale hydrogen production and low-pressure hydrogen pipelines for distribution will be more economical than local production and use of hydrogen [35].

In the future, a trend towards full electric is expected. But also an increase in energy sources providing DC power is expected [36]. The projected increase in the number of DC powered components for residential and industrial application, together with more distributed generation units that generate DC power, reveals that DC microgrid systems will soon be the right candidates for future energy systems [37, 38]. The advantages of low voltage DC grids are higher efficiency, material saving and longer lifespan [39]. Especially because battery and fuel cell in FCEVs, respectively store and produce DC electricity, a DC microgrid is preferred in the CPPP mid-century concept design.

Taking into account all these future developments, a system design for the CPPP was developed, which makes use of a local hydrogen distribution network, an internal DC microgrid and solely FCEV occupation. Figure 8.5 shows a scheme of the CPPP design.

The following system-level assumptions were applied to the CPPP model:

- The starting point is an existing car park to which several technical components are added.
- FCEVs are owned by the individual drivers, and the car park operator acts as the aggregator providing services to the energy market.
- The CPPP operator acquires hydrogen from the local low-pressure hydrogen distribution network.

- Hydrogen is continuously fed directly to the fuel cell of the FCEVs while parked and operating in V2G mode, so the on-board stored hydrogen meant for driving is not used.
- The FCEVs are connected to the DC grid of the car park and deliver DC power back in V2G mode.
- There is one central DC to AC converter, which allows the delivery of AC power at the right voltage to the national AC electricity grid.
- The vehicles adjust their power output according to the signal received from the TSO through the data communication system.

Capacity of the Car Park

The size of the car park is determined by the amount of parking places. More parking places per car park implies more potential capacity to offer to the power system. In the Netherlands there are a total of 210,000 parking places in car parks. This excludes the places near hospitals, parking territories and companies. These parking places are divided amongst circa 500 car parks [17]. This means that on average there are 420 parking places in one car park. This amount is considered as the maximum capacity of the car park under study. The maximum power that the car park can offer ($P_{V2G,max}$) is determined by the amount of occupied parking places (vehicles) times the maximum power output of a FCEV (P_{FCEV}) in stationary mode, as shown in Eq. (8.3).

$$P_{V2G,max} = Vehicles \times P_{FCEV} \tag{8.3}$$

To evaluate the effect of the availability of cars on the energy services that the CPPP system could provide, two different occupation patterns were evaluated; A variable *city car park* occupation pattern based on real world data, and a constant *commercial car park*. The city car park represented a standard car park in The Netherlands, while the commercial car park represented those near airports, large convention centers, hotels and hospitals, which are always operating close to their maximum capacity. This occupation pattern is an almost constant value, approaching the maximum number of parking places. Figure 8.6 shows a plot of the amount of cars during a week that are present in both type of car parks.

The two types of frequency reserves considered, FCR and aFRR, must satisfy the market requirements. For FCR this implies that the reserves need to be available for four consecutive hours and for aFRR the capacity needs to be available only 15 min. Both reserves have a minimum capacity that can be offered equal to 1 MW. While upward and downward aFRR are offered separately, FCR is a symmetrical product. If 1 MW is offered it implies that the power source must be able to increase and decrease the power output with 1 MW. Considering the actual EMS operation of the FCEV, the vehicles cannot start consuming electricity if the CPPP needs to decrease its power output. Thus, to offer FCR and aFRR downwards, the CPPP must offer also electricity.

In order to obtain the occupation pattern of the city car park, data from 7 car parks was collected and averaged. The data set contained the empty parking places

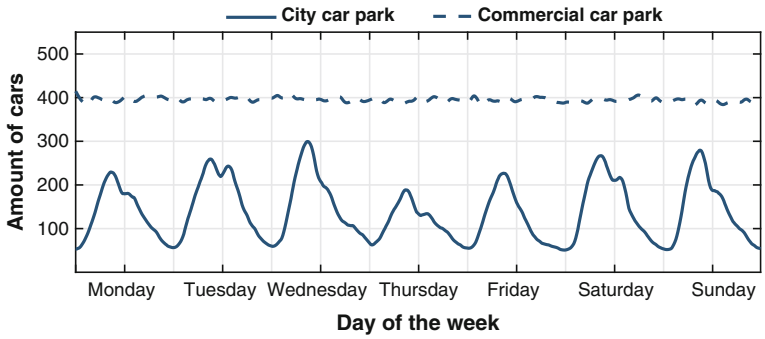

Fig. 8.6 Number of cars that are parked at the car parks during a week for two occupation patterns

measured every 15 min, which is equal to the ISP of the electricity market, and is used as the time step of the simulation.

CPPP Participation in the Electricity Market

Due to the variable available capacity of the vehicles, the forward market is not a reasonable option for the CPPP. The day-ahead and the intraday market, referred to as spot markets, offer enough flexibility for the aggregator to offer its capacity. Almost 90% of the electricity that is sold on the spot markets is sold on the day-ahead market and only 10% is sold on the intraday market. The 2016 prices of the day-ahead market were available on the ENTSO-e transparency platform and were used in the model to calculate the revenues obtained from the offered electricity.

8.2.2.2 Constraints of the System

The total power output of the CPPP was limited by the minimum condition, when all cars were idling, and by the maximum condition ($P_{V2G,max}$), when all cars were offering 10 kW DC. As a consequence also the power that can be offered as electricity (P_e) on the day-ahead market or the reserves offered on the balancing market (P_{FCR}, P_{aFRR}) must remain between those limits, as shown in Eq. (8.4).

$$P_{idling} < P_e, P_{FCR}, P_{aFRR} < P_{V2G,max} \tag{8.4}$$

Based on the amount of electricity that was offered on the day-ahead market, the maximum amount of FCR that could be offered was calculated according to Eq. 8.5.

$$P_{FCR,max} = min((P_e - 0), (P_{V2G,max-P_e})) \tag{8.5}$$

This calculation guarantees the symmetrical characteristics of this particular frequency reserve. However, this amount needed to be available for four consecutive hours. The minimum calculated value in four consecutive hours was assumed as the power reserved for FCR. This value represented the maximum amount of FCR that could be offered by the CPPP. Therefore also 50 and 0% of this value was calculated as an option.

For all the possible combinations of offered electricity and FCR, the amount of aFRR up and down was calculated, as shown respectively in Eqs. (8.6) and (8.7). This was done for all the possible combinations of electricity and FCR offered.

$$P_{aFRR,up} = P_{V2G,max} - (P_e + P_{FCR}) \tag{8.6}$$

$$P_{aFRR,down} = P_e - P_{FCR} - P_{idling} \tag{8.7}$$

The available power in the specific ISP was only considered active if the price for the electricity or the reserves was higher than the marginal costs of the CPPP. To evaluate the effect of the position of the CPPP on the bid ladder a best and worst case marginal cost was calculated based on the hydrogen price and the efficiency of the system.

If the power was active, the amount of energy produced for each product (electricity, FCR, aFRR) was calculated. The amount of electricity offered was the maximum amount it could produce in an ISP. For FCR an approximation was made based on historical data of the frequency in continental Europe. The amount of energy used for aFRR was also based on 2016 historical data of the activated reserves.

8.2.2.3 Revenues and Costs

The total revenues per year (R_{CPPP}) were calculated as the sum of the revenues obtained from the three different products, as shown in Eq. (8.8).

$$R_{CPPP} = R_{e,year} + R_{FCR,year} + R_{aFRR,year} \tag{8.8}$$

The yearly profit for each product is equal to the summation over all the ISPs (N). The amount of required energy per product, in kWh, is multiplied with the respective price, in euro/kWh, for each ISP to obtain the revenues.

The yearly costs (C_{CPPP}) are equal to the operational costs (C_{OC}) of the CPPP summed over the ISP periods in a year, as shown in Eq. (8.9). The latter consist of the cost of purchased energy (C_{pe}), which in this case is the cost of the hydrogen required, and the degradation costs (C_d) the vehicles.

$$C_{CPPP} = \sum_{1}^{N} C_{OC,ISP} = \sum_{1}^{N} (C_{pe,ISP} + C_{d,ISP}) \tag{8.9}$$

Equation 8.10 shows how the cost of the purchased energy was calculated:

$$C_{pe} = m_{H_2} \times p_{H_2} \tag{8.10}$$

where p_{H_2} is the price of hydrogen per kilogram and m_{H_2} is the total amount of hydrogen required. The price for hydrogen at a fueling station is expected to be circa 2 to 4 dollars per kilogram around mid-century, which corresponds to 1.76–3.52 euro per kilogram with an exchange rate of 0.88 euro per dollar [40–43]. Considering a more hydrogen oriented economy and the assumption of a national hydrogen network, it should be possible to buy hydrogen on an industrial scale from the network. The current price for industrially reformed hydrogen from natural gas is around 1 euro per kilogram [44–46]. This value was used for the financially most optimistic case. To calculate the variable costs related to the hydrogen consumption the range of 1.00–3.52 euro per kilogram H_2 was utilized. These values represent, respectively, the best and worst cases considering the hydrogen price and will be used in further sensitivity analysis.

The total mass of hydrogen used by the CPPP for one year was calculated as the sum of the amount of hydrogen consumed for each ISP for all energy products delivered, as shown in Eq. (8.11).

$$m_{H_2} = \sum_{1}^{N} m_{H_{2,ISP}} \tag{8.11}$$

Equation (8.12) shows how the mass of hydrogen for every time step was calculated in the model,

$$m_{H_{2,ISP}} = \frac{E_{V2G,ISP}}{HHV_{H_2} \times \eta_{CPPP,ISP}} \tag{8.12}$$

where $E_{V2G,ISP}$ is the electricity delivered to the grid, $\eta_{CPPP,ISP}$ is the efficiency of the system and HHV_{H_2} is the higher heating value of hydrogen equal to 39.41 kWh/kg. The efficiency is variable and depends on the power output of the vehicles. To estimate the efficiency of the total CPPP system, an average power output per FCEV ($P_{FCEV,ISP}$) in V2G mode was calculated by dividing the total power output of the CPPP (P_{V2G}) by the amount of vehicles that were available in a specific ISP. In this way we assume that all vehicles provide the same amount of power. The efficiency of the total CPPP was assumed equal to the Tank-To-Grid efficiency (TTG) of one FCEV. It represents the efficiency that includes the transformation from hydrogen to the AC electricity that is delivered to the grid. It was calculated with Eq. (8.13), which is the resultant fit from experiments performed with a FCEV in V2G delivering power in the range of 0–10 kW DC [47].

$$\eta_{CPPP,ISP} = \eta_{TTG} = \frac{47 \times P_{FCEV,ISP}}{0.7 + P_{FCEV,ISP}} \tag{8.13}$$

It is expected that the efficiency of the CPPP will increase in the next years because the Tank-to-Wheel efficiency is also expected to increase [26]. The expectation is that the Tank-To-Wheel (TTW) efficiency will increase from 51.5% near future to 61.0% around mid-century. All input variables of this model are based on expected values after 2030. For this reason the CPPP efficiency was increased linearly with the increase of the TTW efficiency. This implies that the used CPPP efficiency in the model was circa 10% higher respect to the one obtained in Eq. (8.13).

The costs for degradation were calculated as extra use of the FCEV due to V2G running time of the fuel cell system. It was assumed that all the electricity was produced by the FC. The degradation of the battery was not taken into consideration. Equation (8.14) shows how the yearly costs for degradation were calculated,

$$C_d = \frac{C_{FC}}{L_h} \times E_{V2G} \times 0.5 \tag{8.14}$$

where, C_{FC} is the cost per kWh (equal to the capital costs per kW of the fuel cell system), L_h is the lifetime in hours, E_{V2G} is the total amount of electricity produced per year, and 0.5 is a factor to correct for uneven degradation because of driving and V2G. In previous research it was assumed that every produced kWh for electricity balancing was causing 50% of the degradation as produced kWh in driving mode [26]. Therefore, the factor of 0.5 is used in the model. As well, using the cumulative produced energy, instead of power or voltage loss as degradation indicator for dynamic operated fuel cells, is in line with other research approaches [48]. For mid-century it is expected that the lifetime of the FC in driving condition will be around 8000 h. The investment costs of a fuel cell system including maintenance are expected to be circa 26.9 euro per kW around mid-century [26].

Marginal Costs of the CPPP

Table 8.1 presents the used values to calculate the marginal costs. The bid price of a power plant was assumed equal to the marginal costs. In the CPPP the total marginal costs were assumed as the sum of the costs of the required hydrogen and the degradation costs to produce one kWh of electricity. During the analysis with the financial model two cases for the marginal costs of the CPPP were considered, which represented a worst case and a best case scenario based on the expected hydrogen price and the efficiency of the CPPP system.

Table 8.1 Overview of the values used to calculate total marginal cost of the CPPP system in the best and worst case scenarios

	H_2 price (€/kg)	Efficiency (%)	Degradation costs (€/kg)	Total marginal costs (€/kg)
Worst case	3.5	40	0.0017	0.2260
Best case	1.0	50	0.0017	0.0524

8.2.2.4 Net Present Value and Payback Time

To calculate the NPV and the payback time, the investment costs were estimated. As it can be seen in Eq. (8.15), the total investment costs (C_{ic}) were equal to the sum of the capital costs (CC_i) of each additional component (n).

$$C_{ic} = \sum_{1}^{n} CC_i \tag{8.15}$$

The payback time (t_{PB}), was calculated as shown in Eq. (8.16),

$$t_{PB} = \frac{C_{ic}}{CF_{years}} \tag{8.16}$$

where C_{ic} are the investment costs and CF_{year} is the yearly cash flow. The latter is the difference between the revenues and the costs and is assumed constant each year. The payback period does not take into consideration the time value of the cash flow and may not present the true picture when it comes to evaluating cash flows of a project. Therefore it is combined with the NPV, which considers the discount rate. To determine the NPV, Eq. (8.17) was used:

$$NPV = \sum_{1}^{L} \frac{CF}{(1+r)^t} \tag{8.17}$$

where CF is the cash flow of each year, t, L is the lifetime of the CPPP and is the discount rate assumed to be 3%. At time t_0 the investment is done, afterwards the yearly cash flow is assumed constant. The NPV is calculated for the worst and best case marginal costs and for different expected lifetimes of the project.

The investment costs represent the adaptations that need to be done to an existing car park to be able to operate as a CPPP with hydrogen as a main power source. This implies that a hydrogen distribution network and a DC grid need to be added to the car park. Also a data communication system needs to be added but the costs of this application are expected to be negligible compared to the other two additions.

Assumptions on the Investment Costs

Every vehicle must be connected with a flexible hose to the local hydrogen network. A vehicle with low-pressure hydrogen inlet for V2G operation has already been proven [49]. Estimating the costs of this system around mid-century is not straightforward as it depends on many factors like the development of the required technologies and the development of the market. Average costs of the nozzle, hose and breakaway ensemble are not publicly available. For this reason we assumed that, due to the characteristic of the transportation and distribution of hydrogen as a gas, it is similar to the transportation and distribution of natural gas in urban areas. This

applied as well for the costs of low/pressure hydrogen distributions systems. The costs for the car park were translated into costs per parking place. The costs per parking place included all the costs related to the local hydrogen distribution system. The costs per parking place were assumed equal to the connection costs with the local gas network for a standard household. This is approximately 900 euro per connection [50, 51]. The DC grid represents the ensemble of the wires and all the converters (DC/DC and AC/DC) required to connect the vehicles to the DC grid and the CPPP to the national electricity grid. Also for this system it is difficult to estimate what the costs will be around mid-century as low voltage DC equipment is currently not yet available on a large scale. There are also no standards yet, regarding low voltage DC networks which makes it difficult to estimate the exact settings of the required components. An increase in the DC low voltage market, as it is expected to occur in mid-century, will stimulate the development of the technology and cause a reduction in costs. The costs to connect the FCEVs to the national electricity grid are estimated to be 1750 euros, equal to current costs for a V2G connection point in a car park. We assumed that these costs included all the components required to operate the FCEV in V2G mode. The calculation of the total investment costs is a rough estimation based on the current costs of similar systems. The sum of the costs for the local hydrogen distribution system and the DC grid are equal to 2650 euro per connected parking place. This gives a total of 1,113,000 euro for 420 parking places. Due to the high uncertainty of this value, it is taken into consideration in the sensitivity analysis.

8.2.2.5 Sensitivity Analysis

The uncertainties introduced by the model assumptions and the values of the inputs were assessed through a sensitivity analysis. The NPV and payback time values were calculated modifying the input parameters in a range of $\pm 10\%$. The input parameters that were adjusted were the hydrogen price, lifetime of the fuel cell system, investment costs per vehicle, day-ahead price, aFRR up price, aFRR down price, FCR price and the maximum amount of connected vehicles in the car park. The sensitivity analysis was performed only for the city car park. To calculate the NPV a lifetime of 15 years was assumed. For both marginal costs scenarios the analysis was performed.

8.3 Results and Discussion

8.3.1 Experimental Analysis of the Reaction Time of the FCEV in V2G

Figure 8.7 shows the DC combined power of the FC and battery during the tests with two different V2G power outputs, 5 and 10 kW DC namely. The sum of the power values does not correspond exactly at all times to the V2G power output. At times, the

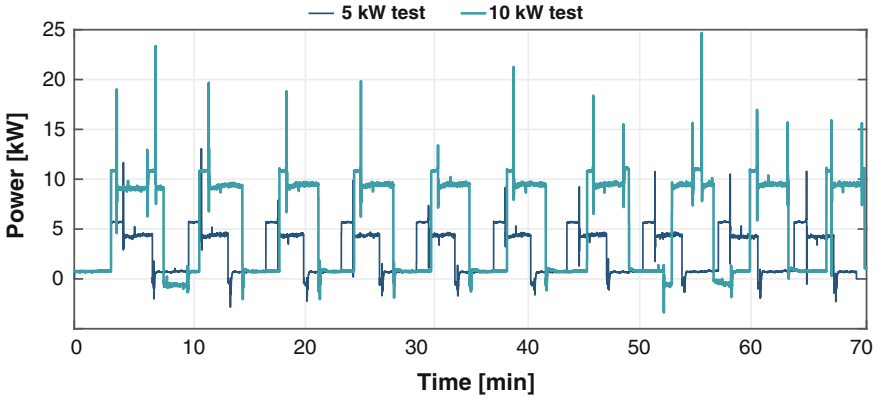

Fig. 8.7 Total DC power supplied by both fuel cell and battery in the FCEV during the dynamic tests

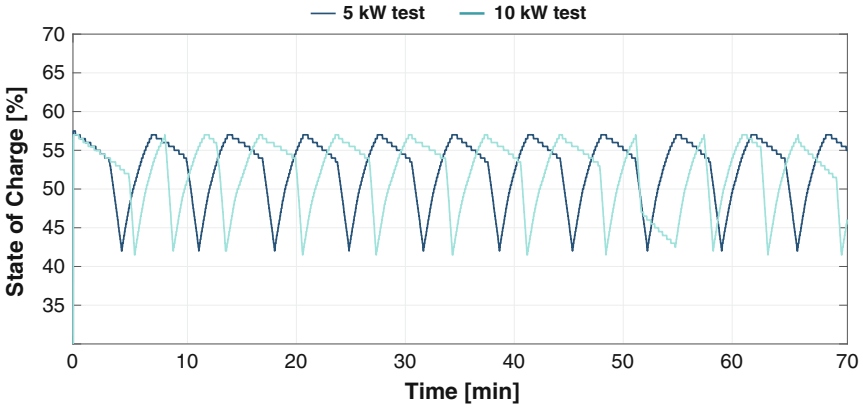

Fig. 8.8 State of charge of the high voltage battery in the FCEV during both tests

sum of battery and FC power is higher than the V2G input signal and other times the value even becomes negative. The reason for this behavior is the Energy Management System (EMS) of the FCEV. The EMS is a crucial part of all EVs. It is the control system, which manages all flows of energy in the car. Every vehicle manufacturer determines different settings in the EMS, which strongly influence the performance of the vehicles. In general the strategy objective in hybrid vehicles, which has a fuel and a battery, is to minimize the fuel consumption. There is, however, a difference between the EMS for driving and V2G mode. Within the Hyundai ix35, when it operates in V2G, the EMS appears to be mainly driven by the state of charge (SoC) of the battery [27]. During both experiments the SoC of the battery always stayed between 42 and 57%, as shown in Fig. 8.8.

To maintain the SoC of the battery within this range, the fuel cell is used to charge the battery. This causes the individual power output of the fuel cell to be higher than

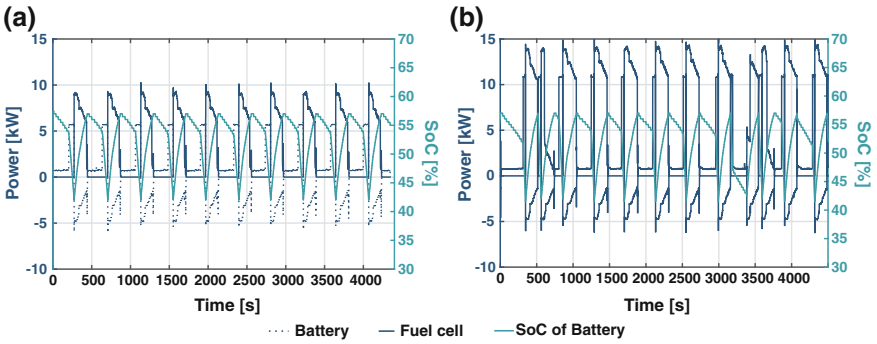

Fig. 8.9 Power flows for fuel cell and battery during the **a** 5 kW and **b** 10 kW DC V2G tests (left y-axis). The State of Charge of the battery is indicated in the right y-axis

the power asked to be delivered to the grid, as can be seen in Fig. 8.9, where the power values for each component are plotted. Negative power values of the battery correspond to periods that the battery was being charged. This is correlated to an increase of the SoC. From Fig. 8.9, the main EMS operations were deduced. When the FCEV was delivering 5 kW DC there was only one mode of operation, which was repeated all 10 times and resulted as follows. During idling, when there was no power requested from the grid, the battery was the main power source that was serving the BoP components. As soon as the car started delivering power to the grid, the battery was providing the power until the SoC reached its lower limit. Then the fuel cell was activated to charge the battery and provide power to the grid as well. Even though the V2G power output was switched off, so the car was not providing power to the grid anymore, the fuel cell was kept on until the battery was charged up 57% SoC. Then the battery remained powering the BoP in idling and this procedure was repeated all test cycles. We refer to this mode of operation as "B+FC", where B stands for battery and FC for fuel cell. On the contrary, there was not a single mode of operation for the ten tests performed when delivering 10 kW DC to the grid, but four different ones. The previously described mode "B+FC" was the most frequent, which occurred in cycles nr. 2, 3, 4, 5, 6, 9 and 10 of the 10 tests performed. In cycle 1, battery was activated first, then FC, then battery again, which was fully drained and at the end the fuel cell was activated one more time ("B+FC+B+FC" mode). In cycle 7 a "B+FC+B" mode was employed to deliver the V2G power. Finally, cycle 8 was the only one that started with the fuel cell delivering power, since the battery was at its lowest SoC. This cycle was "FC+B+FC". Since the power demand is much higher in these tests at 10 kW DC, the alternating behavior between battery and fuel cell to deliver power to the grid is increased and thus results in different modes of operation for each test. They highly depend on the initial state of the battery, because the EMS prioritizes the use of the battery in the SoC range previously mentioned. This mechanism is meant to extend the lifetime of the battery as no deep (dis)charge cycles occur, which is detrimental to the battery's life.

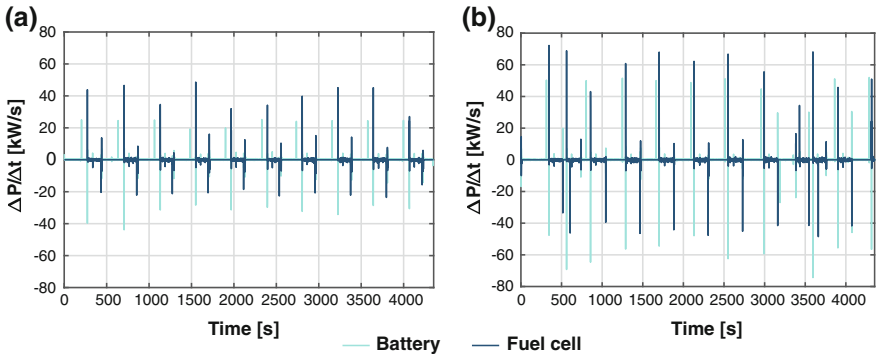

Fig. 8.10 Power gradient versus time for the **a** 5 kW DC tests and the **b** 10 kW DC tests

Table 8.2 Absolute (kW/s) and relative (%/s) upward and downward power gradient values for the fuel cell and battery during the V2G tests

Test	Fuel cell$_{up}$	Battery$_{up}$	Fuel cell$_{down}$	Battery$_{down}$
5 kW	38.3 kW/s (38.3%)	24.7 kW/s (102.8%)	–21.7 kW/s (–21.7%)	–29.6 kW/s (–123.3%)
10 kW	60.2 kW/s (60.2%)	50.0 kW/s (208.2%)	–44.4 kW/s (–44.4%)	–57.2 kW/s (–238.6%)

8.3.1.1 Power Gradient

The power gradient of the fuel cell and the battery measured for the 5 kW and 10 kW DC experiments, are shown respectively in Fig. 8.10a and b. Comparing the results of the two experiments, for higher V2G power settings, the absolute power gradient is higher.

The average of the peak values are shown in Table 8.2 as absolute value and as relative values to the maximum power output of the individual components (100 kW for FC and 24 kW for battery).

It can be observed that for both tests, the absolute power gradient of the fuel cell upward ($FuelCell_{up}$) is higher than the absolute power gradient of the battery upward ($Battery_{up}$). This is not expected since PEMFCs have a lower transient than batteries due to the fact that it is faster to get electricity from stored electrons than drawing hydrogen from the tank, combining it with oxygen and producing the equivalent electricity in the PEMFC [52]. But this observed effect is due to the uneven sizing of the components. That is why we also calculated the relative power gradient. It can be seen that the relative power gradient of the battery is higher for up- and downward regulation than for the fuel cell. For both components, the 10 kW DC experiment had almost a double power gradient compared to the 5 kW DC setting. The current Hyundai ix35 FCEV examined exceeds the performance of a flywheel, which is also considered a suitable device for fast response [53]. For example a 100

Table 8.3 Activation time of the fuel cell and battery in up- and downward reaction in the FCEV when operating in V2G

Test (kW)	Fuel cell$_{up}$ (s)	Battery$_{up}$ (s)	Fuel cell$_{down}$ (s)	Battery$_{down}$ (s)
5	0.13	0.20	0.23	0.17
10	0.17	0.20	0.23	0.17

kW flywheel reaches a full range response in 4 s [54]. This implies that the relative power gradient is 25%/s. This is in most cases a lower gradient than the battery and the FC of the Hyundai ix35. Only when the fuel cell ramps down with a 5 kW DC V2G setting, it presented a lower gradient which was equal to 21.7%/s. This would suggest that for faster response times, the battery would always have to react first and then the fuel cell can provide power for extended periods of time at any of the two power settings.

8.3.1.2 Full Activation Time (FAT)

As can be seen from Table 8.3, the high power gradients result in a sub second reaction time (t_r) of the independent components of the FCEV and thus also for the total V2G power output. The upward reaction time is in the range of 0.13–0.20 s and the downward reaction time results in the range of 0.17–0.23 s. In order to estimate the FAT, the previously obtained reaction time has to be summed to the reaction delay, as was established in Eq. (8.1). A pilot in The Netherlands (NewMotion) was consulted over the reaction delay with aggregated EVs. They offer frequency reserves by increasing or decreasing the charging speed of BEVs. This can be done adapting the software in the charging pole or in the EMS of the vehicle. The reaction delay of these pilots varies strongly depending on the type of aggregation and the used communication system. According to the estimations of the participating pilots, the delay is between 2 and 7 s. The actual maximum allowed reaction delay for FCR is, however, only 2 s. The ability to offer FCR of the aggregated EVs is thus limited due to the relatively long reaction delay. For aFRR the estimated reaction delay is allowed. Since for the FCEV, the reaction time is almost negligible in comparison with the reaction delay, the latter is the one that defines the FAT. The FCEV is certainly able to offer the frequency reserves but the right communication system needs to be adapted to make sure that the reaction delay is small enough.

8.3.2 Financial Analysis

Figure 8.11 presents the results of the yearly cash flow for the different car parks and different power settings offered per car in the car park. The commercial car park has higher yearly cash flows for all cases analyzed than the city car park. This is given

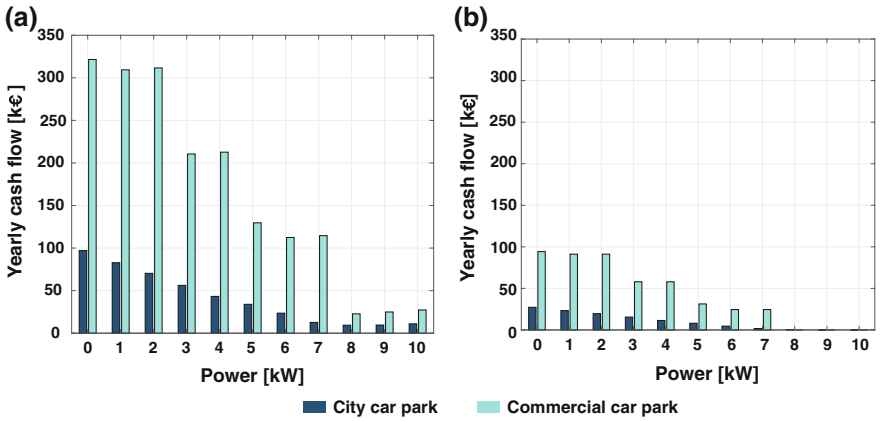

Fig. 8.11 Yearly cash flow results with **a** best and **b** worst case marginal costs for the two types of occupation patterns and considering different values of power for electricity production

Table 8.4 Results of the financial analysis for the two car parks analyzed. The lower limit represents the worst case scenario and higher limit the best case scenario

Type of car park	Yearly cash flow	NPV	Payback time
City	(27–97) k€	(–787–45) k€	(40.8–11.5) years
Commercial	(94–322) k€	(12–2,726) k€	(11.8–3.5) years

the high and constant occupancy of the commercial car park compared to the city car park, where more power capacity from the vehicles is available. In general, when all cars provide higher power, less aFRR can be provided, and this result in lower yearly cash flows. But when lower power is used, competitiveness of the CPPP on the spot market increases, resulting in higher yearly cash flows. The maximum yearly cash flow is obtained when the CPPP offers no electricity and only aFRR upward. As this option is the most profitable, this configuration is assumed for the calculation of the NPV and the payback time. The yearly cash flow, NPV and payback time of the investment of the aggregator to operate as a CPPP system for the two types of occupation patterns are shown in Table 8.4. All of these economic indicators are calculated for the worst and best case for the marginal costs and are expressed in the table as the minimum and maximum limits of the value range, respectively.

The range between worst and best case for the results obtained is very high, indicating how sensible the system is to the marginal costs. The main reason is the lower competitiveness of the car park on the bid ladder for the worst case in comparison with the best case. In general the commercial car park presented a more favorable business case than the city carpark. It can be seen in Table 8.4 that the commercial car park has a payback time that is four times shorter compared to the city car park. The main reason is that there were more moments during the day that the vehicles were parked and could offer reserves. This resulted in higher yearly cash

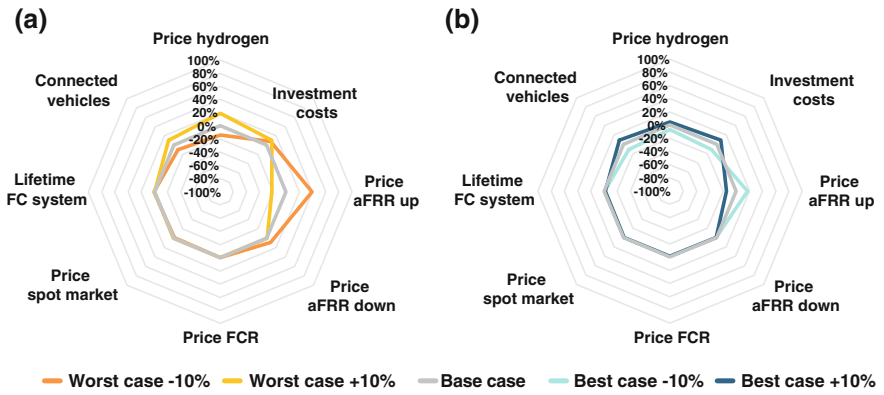

Fig. 8.12 Spider charts showing the results from the sensitivity analysis of the influence of the in put parameters on the payback time for the **a** worst and **b** best case scenarios

flows, and thus shorter payback time. The most interesting investment would result for a commercial carpark with approximately 400 cars available every day. In the best case scenario the investment would be recovered in 3.5 years, obtaining a yearly cash flow of €322,000 and a NPV of €2,726,000.

8.3.2.1 Sensitivity Analysis

Results presented in Sect. 8.3.2 were obtained with a fixed set of assumptions. Additional analysis was conducted to assess how changes in the main input parameters impact the payback time and NPV of the CPPP system. Figure 8.12 shows the effect of varying the input parameters on the payback time for the worst case (Fig. 8.12a) and the best case marginal costs (Fig. 8.12b). The 0% line indicates the outcome with the original values of the parameters. It can be seen that the effect of the price for aFRR down, the price for FCR, the price on the spot market and the lifetime of the FC system on the payback time, is nihil in both cases. The average deviation of the parameters that influence the most the outcome is approximately 10%. These parameters are the investment costs, the amount of vehicles connected, the price for hydrogen and the price for aFRR up.

The amount of connected vehicles is a variable that can be influenced by the aggregator. This is an interesting parameter to adjust to have an influence on the financial potential of the CPPP. A higher occupation, as was seen from the results with the commercial car park, would increase the moments that the aggregator can satisfy the minimum bid size requirement. For city car parks, different incentives could be thought of to favour constant occupation of the car park. This could be done by stimulating users to park longer times by reduced parking tariffs for example. The other three input variables that caused variation in the outputs of the model, were the investment costs, the hydrogen price and the price for aFRR up. The same behavior

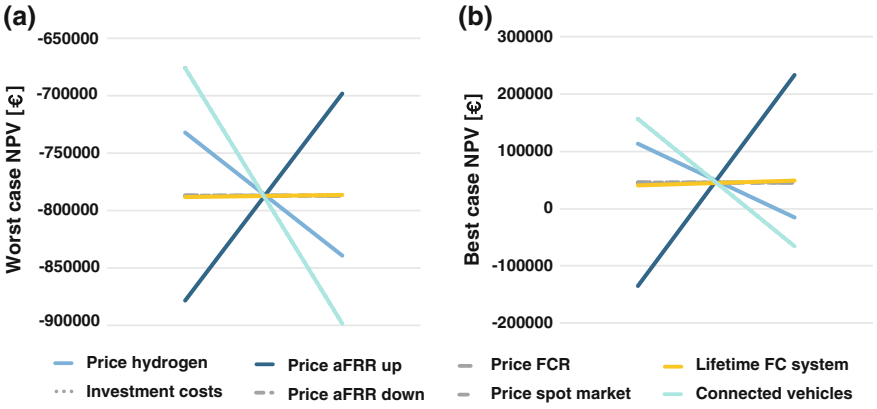

Fig. 8.13 Results from the sensitivity analysis of the effect of the main input parameters on the NPV of the financial analysis

was seen when considering the NPV of the worst and best case for the marginal costs. Results are shown, respectively, in Fig. 8.13a and b (the investment costs data falls exactly under the connected vehicles data). The effect of the changes increased significantly when considering the NPV of the best case for marginal costs. While for all other situations the changes in the outcome were on average $\pm 10\%$, for the best case marginal costs the changes were factor 10 higher. This effect is caused by the fact that the NPV was calculated over a period of 15 years. If the yearly cashflow increases or decreases with 10%, this effect is added to the NPV each year. The occupation pattern of the car park has a large influence on the payback time and the NPV of the aggregator. When considering a constant occupation pattern in the car park, the cash flow of the CPPP could be increased significantly which results in a shorter payback time and higher NPV.

8.4 Conclusions

This research has shown the technical capability and potential income generation that aggregated Vehicle-To-Grid (V2G) services provided with Fuel Cell Electric Vehicles (FCEVs) could have, with focus on the Netherlands. The reaction time of a fuel cell electric vehicle able to provide power to the grid was experimentally tested. An economic analysis was performed for an existing car park owner, acting as aggregator to provide energy services as *Car Park as Power Plant* (CPPP). For this purpose, an in-house developed financial model was used to evaluate the NPV and payback time of a car park acting as aggregator and offering frequency reserves.

The experiments show that both power sources of the fuel cell electric vehicle, which are the fuel cell stack and the battery, are suitable to offer fast frequency

reserves. For the vehicle tested, the ramp up reaction times were in the range of 0.13 - 0.20 s and for ramping down 0.17 - 0.23 s. Besides taking into account the reaction time of the FCEVS, the full activation time (FAT) takes into account the reaction delay in the communication part with aggregator and transmission system operators. The latter was not measured in this research and was obtained from other pilot projects in The Netherlands with battery electric vehicles offering frequency reserves. Both terms together result in values around 2 and 7 s, being the reaction delay the one that defines the FAT. This value is enough to offer automatic frequency restoration reserves (aFRR) but not frequency containment reserves (FCR), since the limit for the latter is 2 s. We recommend for future research/pilot projects to test and improve the communication methods between vehicles and external parties. In this way, the CPPP would be able to increase its frequency reserves portfolio.

This study offered an exploration of the potential economic value that aggregated FCEVs could generate by providing frequency reserves with their fuel cells onboard. The results from the model show that when only the fuel cell stack is used as power source in V2G, the most financial interesting option is to offer only aFRR upwards. Providing this service can yield monetary benefits if the car park has a high and constant occupation. With a car park of approximately 400 cars all year long available, payback times of 11.8 and 3.5 years were obtained taking into account worst and best case scenarios for a 15 year period analysis, respectively. The most sensitive parameters that affect the model results were the amount of vehicles, the price for hydrogen and the price for aFRR up. Future work should be directed at using both power sources in the FCEV, since then there would be more moments that the CPPP could also offer other types of frequency reserves. This would be translated in a higher financial return for the aggregator party.

Acknowledgements C. B. Robledo and A.J.M. van Wijk would like to acknowledge the CESEPS project, which has received funding from the EU Horizon 2020 research and innovation program under the ERA-Net Smart Grids plus grant agreement No 646039, from the NWO and from BMVIT/BMWFW under the Energy der Zukunft program. This work was also financially supported by the Netherlands Organisation for Scientific Research (NWO) [Program "Uncertainty Reduction in Smart Energy Systems (URSES)", Project number 408-13-001] and GasTerra B.V.

References

1. M. Scherer, Frequency control in the European power system considering the organisational structure and division of responsibilities. Ph.D. thesis (2016). https://doi.org/10.3929/ethz-a-010692129Rights
2. P.S. Kundur, N.J. Balu, M.G. Lauby, *Power System Stability And Control*. EPRI Power System Engineering Series (McGraw-Hill, 1994), https://books.google.nl/books?id=v3RxH_GkwmsC
3. M. Huber, D. Dimkova, T. Hamacher, Energy **69**, 236 (2014), http://dx.doi.org/10.1016/j.energy.2014.02.109
4. M.d.l.T. Rodríguez, M. Scherer, D. Whitley, F. Reyer, *IEEE PES General Meeting* (2014). https://doi.org/10.1109/PESGM.2014.6939825

5. W. Kempton, S. Letendre, Transp. Res. Part D: Transp. Environ. **2**(3), 157 (1997). 1361-9209/97 https://doi.org/10.1016/S1361-9209(97)00001-1
6. A. van Wijk, L. Verhoef, Our car as power plant (2014). https://doi.org/10.3233/978-1-61499-377-3-i, http://www.medra.org/servlet/aliasResolver?alias=iospressISBN&isbn=978-1-61499-376-6&spage=7
7. W. Kempton, J. Tomić, J. Power Sour. **144**(1), 280 (2005). https://doi.org/10.1016/j.jpowsour.2004.12.022
8. P. Codani, M. Petit, SSRN (2014). https://doi.org/10.2139/ssrn.2525290
9. M.R. Sarker, Y. Dvorkin, M.A. Ortega-Vazquez, IEEE Trans, Power Syst. **31**(5), 3506 (2016). https://doi.org/10.1109/TPWRS.2015.2496551
10. W. Kempton, J. Tomic, S. Letendre, A. Brooks, T. Lipman, Vehicle-to-grid power: battery, hybrid, and fuel cell vehicles as resources for distributed electric power in California. Technical report, California Air Resources Board and the California Environmental Protection Agency (2001)
11. X. Zhang, S.H. Chan, H.K. Ho, S.C. Tan, M. Li, G. Li, J. Li, Z. Feng, Int. J. Hydr. Energy **40**(21), 6866 (2015). https://doi.org/10.1016/j.ijhydene.2015.03.133
12. IEA, Large-scale electricity interconnection - Technology and prospects for cross-regional networks. Technical report (2016)
13. ENTSO-E, p. 158 (2013)
14. M.J. Poorte, Car park as power plant offering frequency reserves. A technical and economic feasibility assessment. Ph.D thesis, Delft University of Technology (2017)
15. Products, *Day-Ahead Auction* (2018), https://www.epexspot.com/en/product-info/auction
16. Products, *Intraday Continuous* (2018)
17. European Commission, *Reducing CO2 Emissions from Passenger Cars* (2017), https://ec.europa.eu/clima/policies/transport/vehicles/cars_en
18. R.A.C. Van Der Veen, R.A. Hakvoort, *2009 6th International Conference on the European Energy Market, EEM 2009*, pp. 1–6 (2009). https://doi.org/10.1109/EEM.2009.5207168
19. Honda Begins Sales of All-new Clarity Fuel Cell - Clarity Fuel Cell Realizes the World's Top-class Cruising Range Among Zero Emission Vehicles of Approximately 750 km (2016), http://world.honda.com/news/2016/4160310eng.html?from=r
20. Hyundai Motor Company (HMC), *Hyundai ix35 Fuel Cell* (2016), https://www.hyundai.com/worldwide/en/eco/ix35-fuelcell/highlights
21. Hyundai Media Center. NEXO: The Next-Generation Fuel Cell Vehicle From Hyundai (2018), http://www.hyundainews.com/en-us/releases/2456
22. Toyota Motor Corporation (TMC), *Toyota Global Newsroom: Outline of the Mirai* (2014), https://newsroom.toyota.co.jp/en/download/13241306
23. M. Gurz, E. Baltacioglu, Y. Hames, K. Kaya, Int. J. Hydr. Energy **42**(36), 23334 (2017). https://doi.org/10.1016/j.ijhydene.2017.02.124
24. J.K. Kissock, in *Proceedings of the 1998 International Solar Energy Conference* (1998), pp. 121–132
25. T.E. Lipman, J.L. Edwards, D.M. Kammen, Energy Pol. **32**(1), 101 (2004). https://doi.org/10.1016/S0140-6701(04)90146-4, http://linkinghub.elsevier.com/retrieve/pii/S0140670104901464
26. V. Oldenbroek, L.A. Verhoef, A.J.M.V. Wijk, Int. J. Hydr. Energy 1–31 (2017). https://doi.org/10.1016/j.ijhydene.2017.01.155
27. V. Oldenbroek, V. Hamoen, S. Alva, C. Robledo, L. Verhoef, A.V. Wijk, in *6th European PEFC and Electrolyser Forum* (2017), pp. 1–21. 978-3-905592-22-1
28. R. van der Veen, R. Verzijlbergh, Z. Lukszo, A.V. Wijk, in *10th International Conference on Sustainable Energy and Environmental Protection* (2017), pp. 27–30. https://doi.org/10.18690/978-961-286-054-7.15
29. The Green Village (2018), https://www.thegreenvillage.org/about-us
30. T. Lim, B. Ahn, ECS Trans. **50**(2), 3 (2012). https://doi.org/10.1149/05002.0003ecst
31. SAE International, SAE electric vehicle and plug in hybrid electric vehicle conductive charge coupler. Technical report, SAE International (2017), https://saemobilus.sae.org/content/j1772_201710

32. RVO, **2**, 1 (2016), http://www.bovag.nl/data/sitemanagement/media/2013_cijferselektrischvervoertmdecember2013.pdf
33. H. platform, Inbreng H2 Platform voor het Aanvalsplan Duurzame Mobiliteit. Stimulering waterstoftankstations en zero emissie brandstofcel elektrische voertuigen 2018–2022, met doorkijk naar 2030. Technical report (2018)
34. K. Alanne, S. Cao, Renew. Sust. Energy Rev. **1** (2016). https://doi.org/10.1016/j.rser.2016.12.098
35. P.E. Dodds, W. McDowall, Uk Shec (7), 3 (2012)
36. J. Woudstra, P. van Willigenburg, B. Groenewald, H. Stokman, S. De Jonge, S. Willems, in *2013 Proceedings of the 10th Industrial and Commercial Use of Energy Conference* (2013), pp. 2–7, http://ieeexplore.ieee.org/xpls/abs_all.jsp?arnumber=6761675
37. J.J. Justo, F. Mwasilu, J. Lee, J.W. Jung, Renew. Sust. Energy Rev. **24**, 387 (2013). https://doi.org/10.1016/j.rser.2013.03.067, http://dx.doi.org/10.1016/j.rser.2013.03.067
38. A.T. Elsayed, A.A. Mohamed, O.A. Mohammed, Electr. Power Syst. Res. **119**, 407 (2015). https://doi.org/10.1016/j.epsr.2014.10.017
39. P. Van Willigenburg, J. Woudstra, T. De Lange, H. Stokman, *Proceedings of the 22nd Conference on the Domestic Use of Energy, DUE 2014* (2014). https://doi.org/10.1109/DUE.2014.6827758
40. International Energy Agency, Technology roadmap. Hydrogen and fuel cells. Technical report (2015), http://www.springerreference.com/index/doi/10.1007/SpringerReference_7300
41. Tractebel Engineering S.A., Hinicio, **228** (2017), http://www.fch.europa.eu/sites/default/files/P2H_Full_Study_FCHJU.pdf
42. A.J. van Wijk, The green hydrogen economy in the Northern Netherlands. Technical report (2017)
43. J. Eichman, A. Townsend, J. Eichman, A. Townsend (2016)
44. N. Sulaiman, M.A. Hannan, A. Mohamed, E.H. Majlan, W.R. Wan, Daud. Renew. Sust. Energy Rev. **52**, 802 (2015). https://doi.org/10.1016/j.rser.2015.07.132
45. S. Dillich, T. Ramsden, M. Melaina, Hydrogen production cost using low-cost natural gas. Technical report (2012)
46. Energy Renaissance (2018), http://www.h2energyrenaissance.com/
47. C.B. Robledo, V. Oldenbroek, F. Abbruzzese, A.J. van Wijk, Appl. Energy **215**(2017), 615 (2018). https://doi.org/10.1016/j.apenergy.2018.02.038
48. M. Jouin, M. Bressel, S. Morando, R. Gouriveau, D. Hissel, M.C. Péra, N. Zerhouni, S. Jemei, M. Hilairet, B. Ould, Bouamama. Appl. Energy **177**, 87 (2016). https://doi.org/10.1016/j.apenergy.2016.05.076
49. C.B. Robledo, V. Oldenbroek, J. Seiffers, M. Seiffers, A. van Wijk, in *2017 Fuel Cell Seminar and Energy Exposition* (2017), pp. 7–9
50. A. van Wijk, C. Hellinga, Hydrogen - the key to the energy transition. Technical report (2018), http://edepot.wur.nl/333952
51. Liander. Liander. Tarieven 2017 voor consumenten. (2017), https://www.liander.nl/consument/aansluitingen/tarieven2017/?ref=14389
52. J. Wishart, Fuel cells versus batteries in the automotive sector. Technical report (2014)
53. Beacon Power, Frequency regulation compensation in the safe harbor statement. Technical report (2010), https://www.ferc.gov/EventCalendar/Files/20100526085637-Judson,BeaconPower.pdf
54. M. Lazarewicz, *Flywheel Technology Energy Storage for Grid Services Safe Harbor Statement* (2011), https://www.uml.edu/docs/15_Energy_M_Lazarewicz_tcm18-48972.pdf